

## Influence of droplet characteristics on the electrochemical behavior of Zinc

G A. EL-Mahdy\*, Amro K.F. Dyab, Ayman M. Atta, Hamad A. Al-Lohedan

King Saud University, Chemistry Department, College of Science, P.O.Box - 2455, Riyadh - 11451, Saudi Arabia

\*E-mail: [gamalmah2000@yahoo.com](mailto:gamalmah2000@yahoo.com)

Received: 16 May 2013 / Accepted: 18 June 2013 / Published: 1 July 2013

---

The time-dependent corrosion rate, droplet height, volume loss and contact angle were monitored during the course of evaporation of a single droplet of NaCl on zinc surface. The results show that contact angle and droplet height decrease linearly with increasing droplet holding time, while volume loss increases. Experimental results indicated that the outmost surface of the droplet is fixed during the last stage of evaporation without changing the location of edge. The evaporation process of a single droplet can be divided into two stages. It begins from the droplet surface and continued during the second drying stage with increasing the amount of corrosion products. The mechanism zinc corrosion under a single droplet of NaCl will be proposed and discussed.

---

**Keywords:** Zinc, contact angle, corrosion rate, EIS

### 1. INTRODUCTION

Zinc is one of the most used metals in electroplating and is generally used as sacrificial anode in cathodic protection of steel against corrosion. The atmospheric corrosion of zinc has been studied in field exposures as well as in laboratory with controlled environments [1–14]. It was reported previously that zinc hydroxide chloride and zinc oxide are the dominant corrosion products [1]. Kalinauskas et al [15] noticed the formation of zinc hydroxide carbonate or hydrozincite;  $(Zn_5(OH)_6(CO_3)_2H_2O)$  during the exposure in NaCl solution [16]. The effect of NaCl,  $Na_2SO_4$ ,  $NH_4Cl$  and  $(NH_4)_2SO_4$  nuclei has been investigated on zinc corrosion at 40°C and 85% RH [17]. The results showed that the loss of zinc decreased in the order  $NH_4Cl > NaCl > Na_2SO_4 > (NH_4)_2SO_4$ . Patterson and Wilkinson [18] also investigated the effect of NaCl and  $NH_4Cl$  particles on zinc corrosion at 20°C and 80% RH. They indicated that the corrosion of zinc in the presence of NaCl was greater than that in the presence of  $NH_4Cl$ . The time of wetness (TOW) can be defined as the period during which a metallic surface is covered by adsorptive and/or liquid film of electrolyte, necessary for initiation and

progress of the atmospheric corrosion, which can be measured or calculated [19-20]. The study of the wetting of metal surfaces is important in order to understand the process controlling atmospheric corrosion [21– 25]. A metal runoff process [26–34] is defined as liberation of metal ions from the corroded surface to the environment. It was reported that roofs made from galvanized hot dip steel generated zinc runoff precipitations of 1–44 g m<sup>-3</sup>, while roofs made from zinc generated zinc concentrations between 0.01 and 2.6 g m<sup>-3</sup> [35]. Despite the extensive amount of work reported on the atmospheric corrosion of zinc, there is still a lack of study on the electrochemical behavior of zinc under a single droplet of NaCl. The aim of the present work was to examine the corrosion process of zinc under a single droplet of NaCl using a recently developed an experimental set-up [36]. The mechanism of zinc corrosion under a single droplet of NaCl will be discussed.

## 2. EXPERIMENTAL PROCEDURE

### 2.1 Electrochemical impedance spectroscopy (EIS)

EIS impedance measurements were performed using a Solartron 1470E system (potentiostat/galvanostat ) with Solartron 1455A as frequency response analyzer. Multistate software was used to run the tests and collect the experimental data. EIS experiments were measured in frequency at 10kHz and 0.01 mHz with perturbation amplitude of 10 mV. Testing electrolyte of 0.5 M NaCl aqueous solution was prepared by dissolving NaCl in deionized water. The polarization resistance ( $R_p$ ) was determined by subtracting the high frequency impedance at 10 kHz from the low frequency impedance at 10 mHz.

### 2.2. Material and electrode preparation

Two-electrode cell configuration was fabricated from zinc sheet (99.99) with dimensions 1mm (width) and 10 mm (length) and embedded parallel in an epoxy resin with 0.1 mm apart from each other. Prior to experiments, the electrode was polished with SiC emery paper down to #2000. The cell containing the two metal plates was set horizontally on an acrylic vessel with the metal surface facing upwards.

### 2.3. Monitoring the droplet characteristics

The changes in contact angle, volume loss and droplet height during the progress of corrosion process will be monitored using a drop shape analysis system (DSA-100, Kruss, Germany) with analysis software DSA4 software (V.1.0-03).

### 3. RESULTS AND DISCUSSION

#### 3.1 Monitoring the Volume loss and the droplet height

Figure 1 shows the droplet shape at different holding times. The monitoring data for the volume loss and the droplet height during the course of droplet evaporation is shown in Figures 2 and 3, respectively. It can be seen that the volume loss increases while, the droplet height decreases linearly with time as a result of the droplet evaporation as holding time progresses. The volume loss or the evaporation process can be divided into two stages.

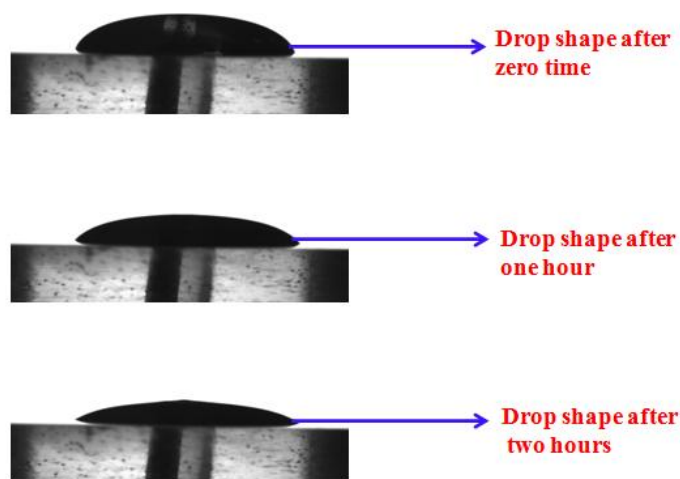


Figure 1. Droplet shape at different holding times.

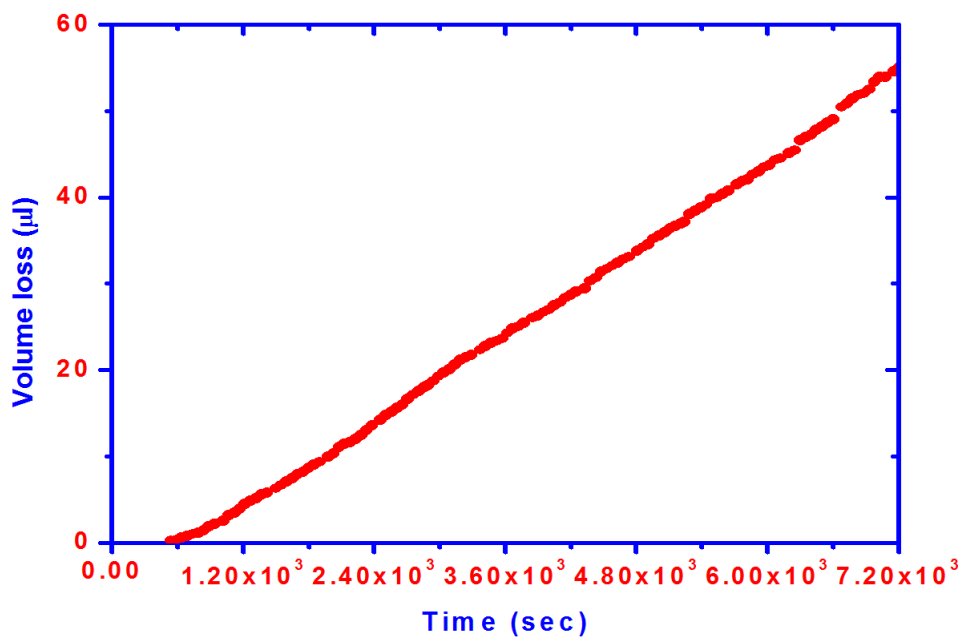
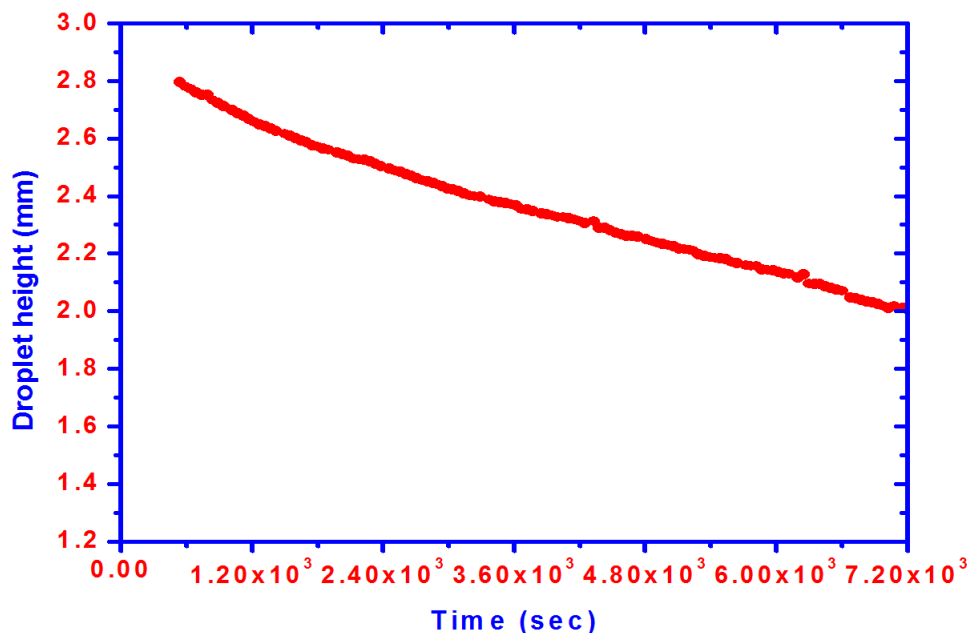


Figure 2. Monitoring data of volume loss with droplet holding time



**Figure 3.** Monitoring data of droplet height with droplet holding time

The droplet initially has greatest amount of liquid when it enters the drying medium during the initial stage of evaporation. The evaporation of liquid begins from the droplet surface owing to gaining sensible heat from surrounding environment. During the second drying stage, the droplet height decreases and the thickness of the corrosion products continuously increases, while the diameter of the contact area remains constant. It is clear that during the last stage of evaporation, the corrosion process inside the droplet became similar to the corrosion process occurred under thin electrolyte layers with different rates of evaporation in radial and vertical directions. It is generally expected that the evaporation process occurs fast as the droplet surface area contact with air becomes large. It can be seen that the outmost surface (edge) of droplets is fixed during last stage of evaporation just before being dried out, without changing the location of edge as shown in Fig. 1.

### 3.2 Monitoring of contact angle

Contact angles play an important role in the interaction of the liquid with exposed surface and gives information about hydrophilicity or hydrophobicity of a surface. Contact angle of the droplet is closely related to the electrochemical properties of liquid/metal interface. Changes in contact angle with holding time are shown in Fig. 4 for a single droplet of 0.5M NaCl placed gently on zinc surface. In general, contact angle decreased with increasing holding time. It seems that the dissolution of zinc give rise to charges attached on the metal surface, leading to the decrease of liquid-metal interfacial energy and the acceleration of the water evaporation from primary-droplet, which might causes a changes in the corrosion rate. Therefore, it is reasonable to conclude that the low wettability observed during the initial stage exhibit low corrosion rate, while high wettability exhibits high corrosion rate. The deposition of corrosion products as well as NaCl crystals may form an insulating layer, which acts

as a new substrate and give rise to more error in contact angle measurements especially during the last stage of monitoring.

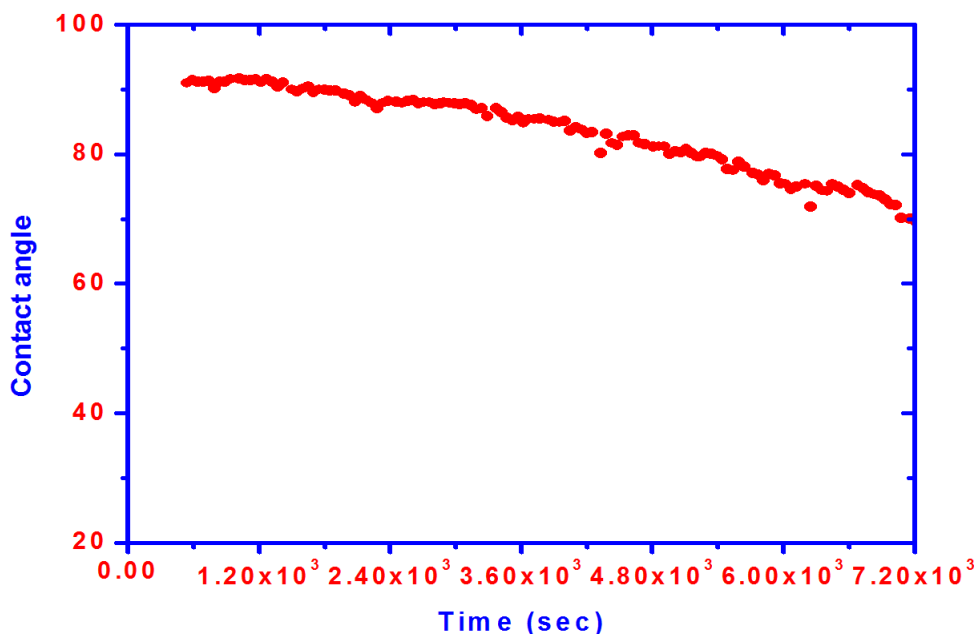


**Figure 4.** Variations of contact angle with droplet holding time.

### 3.3. Monitoring the corrosion rate of zinc

The polarization resistance ( $R_p$ ) is monitored continuously versus the droplet holding time and the data is shown in Fig. 5. The polarization resistance  $R_p$  can be calculated using electrochemical impedance measurements (EIS) by measuring at two different frequencies:  $Z_H$  (high frequency of about 10 kHz) and  $Z_L$  (low frequency of about 10 mHz) [36-45]. The reciprocal of  $R_p$  ( $1/R_p$ ) is proportional to the corrosion rate and can be determined from the following equation [46]:

$$I_{corr} = k/R_p \tag{1}$$

Where  $k$  is constant and is given by:

$$K = \frac{b_a \cdot b_c}{2.303(b_a + b_c)} \tag{2}$$

where  $b_a$  and  $b_c$  represent anodic and cathodic Tafel slope, respectively. The value of  $K$  is a function of metal and electrolyte [45] and can be assumed to be constant for a given metal/electrolyte system. The reciprocal of  $R_p$  ( $1/R_p$ ), which is proportional to the corrosion rate increases slowly during the initial stage of monitoring and rapidly increases with increasing holding time during the last stage of monitoring. The corrosion process under a single droplet can be classified in two distinct regions. The corrosion process of zinc experiences in the first region during the initial stage of monitoring is slow and is anodically controlled by zinc dissolution, which is similar to the behavior in

of zinc in bulk solution, while droplet height is high. The rapid increase in corrosion rate observed during the last stage of monitoring changes from an anodically controlled process (high droplet height) during the initial stage of monitoring (limited oxygen diffusion) to cathodic controlled process of oxygen reduction (low droplet height). Hence, it permits gases to diffuse faster to the surface resulting in an increase in the cathodic reduction of oxygen and increasing the corrosion rate during the last stage of monitoring.

### 3.4. Mechanism of Zinc corrosion under a single droplet of NaCl

The mechanism of zinc under a single droplet of NaCl can be described in two stages. Zinc dissolved during the initial stage in NaCl according to:



In this stage the corrosion of zinc is controlled by zinc dissolution.

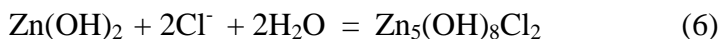
As the droplet holding time progresses the cathodic reaction occurs during the last stage of monitoring as:



As the droplet holding time progresses zinc hydroxide ( $\text{Zn}(\text{OH})_2$ ) will be produced from the reaction of  $\text{Zn}^{2+}$  with  $\text{OH}^-$  as :



Zinc hydroxide chloride  $\text{Zn}_5(\text{OH})_8\text{Cl}_2$  [15] will be formed as the droplet height decreases as a result of water evaporation during the last stage of monitoring according to:



During the last stage of monitoring there is possibility for the formation of zinc hydroxide carbonate ( $\text{Zn}_5(\text{OH})_6(\text{CO}_3)_2$ ) [16].

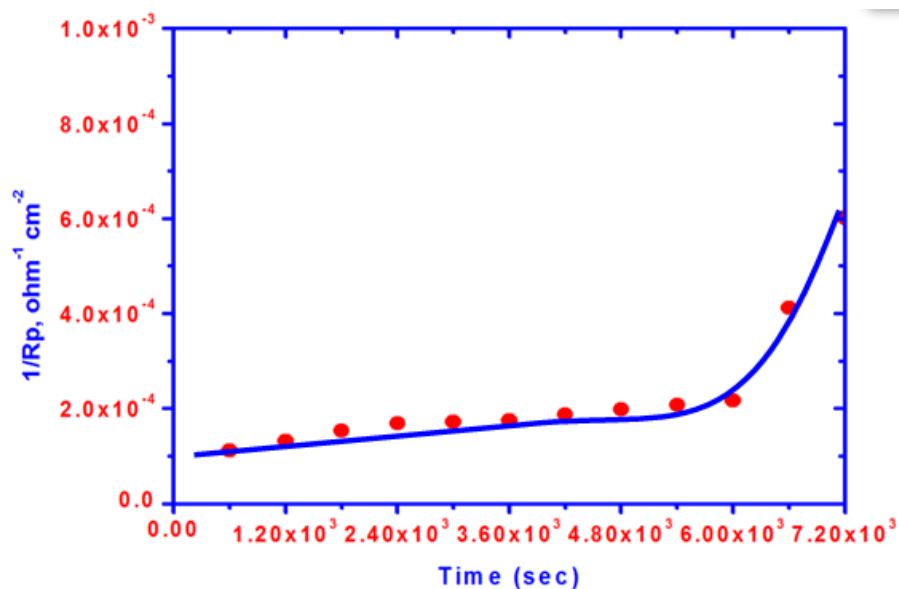
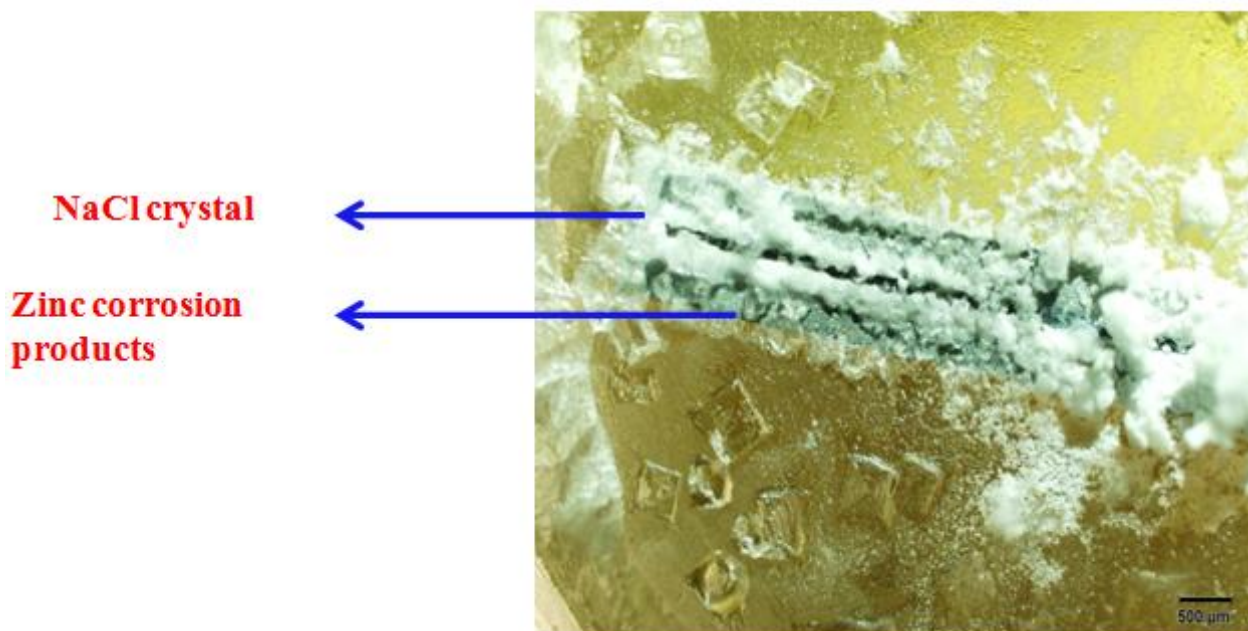


Figure 5. Monitoring data of corrosion are with droplet holding time



**Figure 6.** Droplet shape after complete drying

It is evident that the mechanism of zinc corrosion changed from anodically controlled by zinc corrosion during the initial stage of corrosion (equation 3) to cathodically controlled by a reduction of oxygen as the droplet height decreases during the last stage of monitoring (equation 4). The higher corrosion rate observed during the last stage of monitoring shown in Fig. 5 can be attributed to a decrease in droplet height as a result of water evaporation, which provides a shorter path for oxygen diffusion. Hence, enhances the corrosion rate during the last stage of monitoring. After complete drying corrosion products will be formed and entirely covered the surface with the formation of zinc corrosion products as well as NaCl crystals as shown in Fig.6. It can be concluded that the corrosion mechanism proceeds through dissolution–precipitation mechanism under a single droplet of NaCl. The mechanism commences with the formation of distinct anodes and cathodes under the droplet during initial stage of monitoring. As the droplet holding time progresses the volume loss of electrolyte increases followed by a reduction of oxygen during the evaporation of electrolyte. Ionic species migrate in the droplet solution and eventually precipitated as corrosion products after complete drying during the last stage of monitoring as shown in Fig. 6.

#### 4. CONCLUSIONS

1- The contact angle and droplet height decrease linearly with increasing droplet holding time, while volume loss increases.

2- Experimental results indicated that the outmost surface of the droplet is fixed during the last stage of evaporation without changing the location of edge.

3- The evaporation of liquid begins from the droplet surface and continued during the second drying stage with an increase in the amount of corrosion products.

4- The mechanism zinc corrosion under a single droplet of NaCl proceeds through dissolution – precipitation mechanism.

#### ACKNOWLEDGMENT

The authors extend their appreciation to the Deanship of Scientific Research at King Saud University for funding this work through research group no RGP-VPP-235.

#### References

1. M. Benarie, F.L. Lipfert, *Atmos. Environ.* 20 (1986) 1947.
2. J.J. Friel, *Corrosion* 42 (1986) 422.
3. J.E. Svensson, L.G. Johansson, *J. Electrochem. Soc.* 140 (1993) 2210.
4. J.E. Svensson, L.G. Johansson, *Corros. Sci.* 34 (1993) 721.
5. R. Lindström, J.E. Svensson, L.G. Johansson, *J. Electrochem. Soc.* 147 (2000) 1751.
6. T. Falk, J.E. Svensson, L.G. Johansson, *J. Electrochem. Soc.* 145 (1998) 39.
7. T. Falk, J.E. Svensson, L.G. Johansson, *J. Electrochem. Soc.* 145 (1998) 2993.
8. T.E. Graedel, *J. Electrochem. Soc.* 136 (1989) 204c.
9. S.G. Lee, S.G. Kang, *J. Materi. Sci. Lett.* 16 (1997) 902.
10. T.E. Graedel, *J. Electrochem. Soc.* 136 (1989) 193.
11. E. Almeida, M. Morcillo, B. Rosales, *Br. Corros. J.* 35 (2000) 284.
12. E. Almeida, M. Morcillo, B. Rosales, *Br. Corros. J.* 35 (2000) 289.
13. A.K. Neufeld, I.S. Cole, A.M. Bond, S.A. Furman, *Corros. Sci.* 44 (2002) 555.
14. Q. Qu, C.W. Yan, Y. Wan, C.N. Cao, *Corros. Sci.* 44 (2002) 2789.
15. Q. Qu, L. Li, W. Bai, C. Yan, C.N. Cao, *Corros. Sci.* 47 (2005) 2832–2840.
16. P. Kalinauskas, I. Valsiunas, M. Samuleviciene, E. Juzeliunas, *Corros. Sci.* 43 (2001) 2083.
17. B. Sanyal, D.V. Bhadwar, *J. Sci. Ind. Res.* 21D (1962) 243.
18. W.S. Patterson, J.H. Wilkinson, *J. Soc. Chem. Ind.* 57 (1938) 445.
19. ISO 9223:92 Corrosion of metals and alloys, Corrosivity of atmospheres, Classification, ISO Int., Geneva, 1992.
20. ASTM Practice G84-89: ‘Standard practice for measurement of time-of wetness on surfaces exposed to wetting conditions as in atmospheric corrosion testing’, West Conshohocke, PA, ASTM Int., 1989.
21. K. Barton, Z. Bartonova, *Mater. Corros.* 21 (1970) 85.
22. I.S. Cole, R. Holgate, P. Kao, W. Ganther, *Corros. Sci.* 37 (1995) 455.
23. J. Tidblad, A.A. Mikhailov, V. Kucera, *Protect. Metals* 36 (2000) 533.
24. I.S. Cole, W.D. Ganther, D.A. Paterson, A. Bradbury, *Corros. Eng. Sci. Technol.* 40 (2005) 328.
25. A. Nishikata, Y. Ichihara, T. Tsuru, *Corros. Sci.* 37 (1995) 897–911.
26. J.W. Spence, F.H. Haynie, F.W. Lipfert, S.D. Cramer, L.G. McDonald, *Corrosion* 48 (1992) 1009.
27. I.W. Odnevall, P. Verbiest, W. He, C. Leygraf, *Corros. Sci.* 42 (2000) 1471.
28. S. Bertling, I. Odnevall, C. Leygraf, D. Berggren, in: H.E. Townsend (Ed.), *Outdoor Atmospheric Corrosion*, ASTM STP 1421, ASTM Int., West Conshohocken, PA, 2002, pp. 200–215.
29. W. He, I. Odnevall, C. Leygraf, in: H.E. Townsend (Ed.), *Outdoor Atmospheric Corrosion*, ASTM STP 1421, ASTM Int., West Conshohocken, PA, 2002, pp. 216–229.
30. J.H. Sullivan, D.A. Worsley, *Br. Corros. J.* 39 (2002) 282–288.
31. S. Matthes, S. Cramer, S. Bullard, B. Covino, G. Holcomb, in: *Proceedings of the 58th Annual Conference Corrosion*, 2003 NACE, Paper 03598.
32. S. Jouen, B. Hannoyer, A. Barbier, J. Kasperek, M. Jean, *Mater. Chem. Phys.* 85 (2004) 73.
33. D. Reiss, B. Rihm, C. Thoni, M. Faller, *Water Air Pollut.* 150 (2004) 101.

34. I.W. Odnevall, P. Verbiest, W. He, C. Leygraf, *Corros. Sci.* 42 (2000) 1471.
35. A. Askey, S.B. Lyon, G.E. Thompson, J.B. Johanson, G.H. Wood, P.W. Sage, M.J. Cooke, *Corros. Sci.* 34 (1993) 1055.
36. G. A. EL-Mahdy<sup>1</sup>, Amro K.F. Dyab<sup>1</sup>, Hamad A. Al-Lohedan<sup>1</sup> *Int. J. Electrochem. Sci.*, 8 (2013) 5232.
37. G.A. El-Mahdy, A. Nishikata, T. Tsuru, *Corros. Sci.* 42 (2000) 183.
38. G.A.EL-Mahdy, A.Nishikata and T.Tsuru *Corros. Sci.* (UK) 42 (2000) 1509.
39. G. A. EL – Mahdy and Kwang B. Kim *Corrosion* 63 (2007) 171.
40. G. A. EL-Mahdy and Kwang B. Kim *Electrochemistry* 75 No. 5 (2007).
41. G. A. EL – Mahdy *Corros. Sci.* 47 (2005) 1370.
42. G. A. EL – Mahdy *J. App. Electrochem.* 35 (2005) 347.
43. G. A. EL – Mahdy and Kwang B. Kim *Corrosion* 61 (2005) 420
44. G. A. EL – Mahdy and Kwang B. Kim *Electrochim. Acta* 49 (2004) 1937.
45. G.A. El-Mahdy, *Corrosion* 59 (2003) 505.
46. M. Stern, A.L. Geary, *J. Electrochem.* 104 (1957) 56.